Integrated spectral mapping of precious and base metal-related mineral footprints, Nanjilgardy Fault, Western Australia

by

MA Wells*, C Laukamp*, and EA Hancock

The northern margin of the Capricorn Orogen, encompassing the northern boundary of the Ashburton Basin, represents one of the major Paleoproterozoic gold provinces within Australia (Şener et al., 2005), along which a number of gold deposits are situated nearby to major, possibly mantle-tapping, regional structures, such as the Baring Downs and Nanjilgardy Faults (Fig. 1). These recently interpreted, large-scale structures are considered to form a deep-seated plumbing system, focusing fluid flow and energy flux from the mantle into the upper crust (Johnson et al., 2013), that may have given rise to a number of polymetallic, mineral systems known throughout the region (e.g. Pirajno, 2004; Tyler et al., 2011).

The Nanjilgardy Fault (NF) juxtaposes an inlier of the Proterozoic Shingle Creek Group (formerly lower Wyloo Group) and older metasedimentary units against the Wyloo Group (formerly upper Wyloo Group) at the Mt Olympus gold deposit (Fig. 1). Gold mineralization at Mt Olympus is hosted within coarse- and fine-grained, epiclastic sedimentary rocks (sandstone/siltstone) of the Mt McGrath Formation and also within the Duck Creek Dolomite (Şener et al., 2005) (Fig. 1). Mineralization is associated with strong sulfide alteration, but is not correlated with either whole-rock sulfide content or any quartz veining (Morant and Doepel, 1997). The alteration mineralogy consisting of quartz–sericite–carbonate (e.g. Morant and Doepel, 1997; Piranjo, 2004; Şener et al., 2005) and that detected in the current study (sulfate–white mica–kaolinite–dickite), are strongly spectrally active in the shortwave infrared (SWIR; 1.0 – 2.5 µm) and thermal infrared (TIR; 6.5–14 µm) wavelength ranges.

As part of the Exploration Incentive Scheme (EIS), 24 historical diamond cores (Sipa Resources) drilled along strike of the northwest-southeast trending NF were scanned using the HyLogger-3 system to identify the host rock and alteration mineral assemblage. By combining proximally derived HyLogging-3 data with remotely sensed (e.g. ASTER) data, and validating the identified mineralogy by independent techniques (e.g. X-ray diffraction and geochemical analyses), a spectrally derived, 3D mineral map was developed to better characterize the gold-related alteration mineralogy at Mt Olympus from the deposit scale through to surface expression at the regional scale. These objectives concord with the overarching aim of the Capricorn Distal Footprints project to recognize the mineral signature of concealed ore deposits (Hough, 2015) and adds value to the Geological Survey of Western Australia's (GSWA) precompetitive drillcore hyperspectral data.

* CSIRO, Mineral Resources, Australian Resources Research Centre, Kensington WA 6151

Corresponding author: martin.wells@csiro.au

Deposit-scale alteration mineralogy

Evaluation of historical company (i.e. Sipa Resources) lithological logging and gold assay values, and extraction of the most abundant mineral groups (e.g. white mica, chlorite, kaolin, quartz, and carbonate abundances) using spectral mineral indices derived by processing of the raw HyLogging-3 data, enabled the scanned drillholes to be classed into four gold mineralization groups. These groups comprise: (1) oxidized high-grade types, (2) oxidized primary low-grade types, (3) unoxidized primary types, and (4) proximal and distal low-grade types, all of which are associated with distinct alteration footprints.

Minerals identified hyperspectrally and mapped using the HyLogger-3, validated by XRD analysis, include: muscovite (subordinate phengite); Fe/Mg-chlorite; kaolinite (with variable crystallinity); dickite; pyrophyllite; K/Na-alunite; K-jarosite; quartz; carbonates (dolomite and siderite); and 'opaques', likely to be sulfides (mainly pyrite), and minor carbon. Potential hydrothermal alteration phases in common rock types along the Nanjilgardy Fault were interpreted as: (proximally) Na/K-alunite, well-ordered kaolinite, dickite and pyrophyllite (indicative of advanced argillic alteration); muscovite (indicative of phyllic alteration); Fe/Mg-chlorite and carbonate (distally).

Changes in the alteration mineralogy were better visualized as downhole plots where mineral specific spectral indices mapped the spatial association to reported gold grades (Fig. 2a). For example, in drillhole MOD4 which is representative of an oxidized, high-grade mineralization type, the sulfate species changes from jarosite associated with mineralization, to locally Na/K-alunite away from the mineralized zone (Fig. 2a).

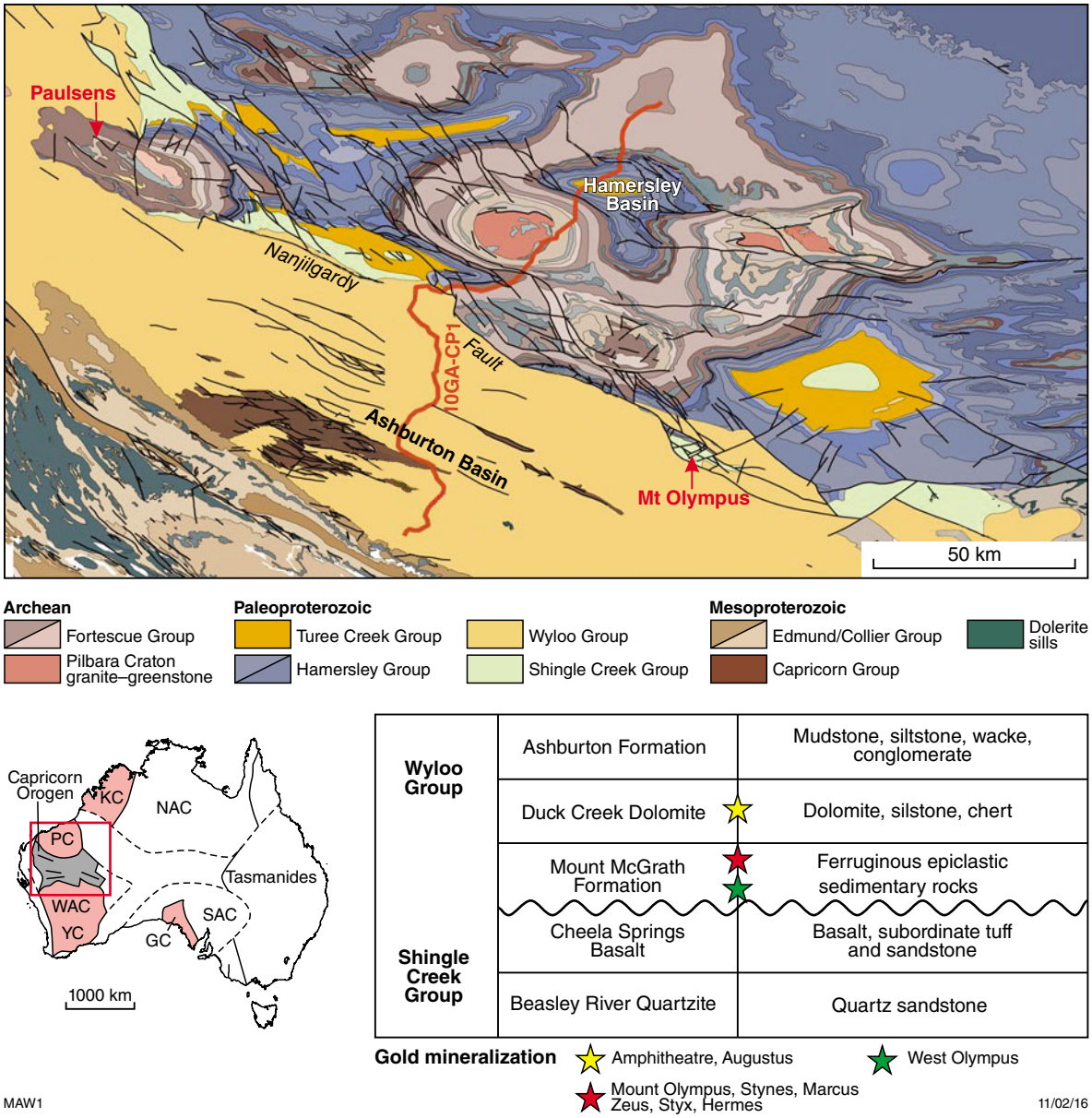

Figure 1. Regional geological setting of the Capricorn Orogen, location of the Nanjilgardy Fault and the Paulsens and Mt Olympus gold deposits. Location of one of the Capricorn Orogen seismic lines, 10GA-CP1 (red line), across the Nanjilgardy Fault is also shown. Regional stratigraphy of the Shingle Creek and Wyloo Groups show that gold mineralization at Mt Olympus is hosted mainly by metasedimentary rocks of the McGrath Formation and the Duck Creek Dolomite (modified from Tyler and Thorne, 1990).

Kaolinite occurs with alunite or is the dominant SWIR-active mineral between sulfate-rich layers. More distally, kaolinite is replaced by dickite and muscovite (Fig. 2a).

Integration of mineral data across drillholes in the vicinity of Mt Olympus allowed the spatial variation in alteration mineralogy to be evaluated at the deposit scale (Fig. 2b), which identified:

- several irregular, poddy, southeast-plunging zones of >0.5 ppm Au (including the largest, now depleted by mining) intersected by the Zoe Fault, the most significant structural feature in the area
- that sulfate alteration was proximal to mineralization on the northern side of the openpit
- that white-mica composition varied from Al-poor proximally to Al-rich distally with respect to gold mineralization
- that chlorite was distally developed.

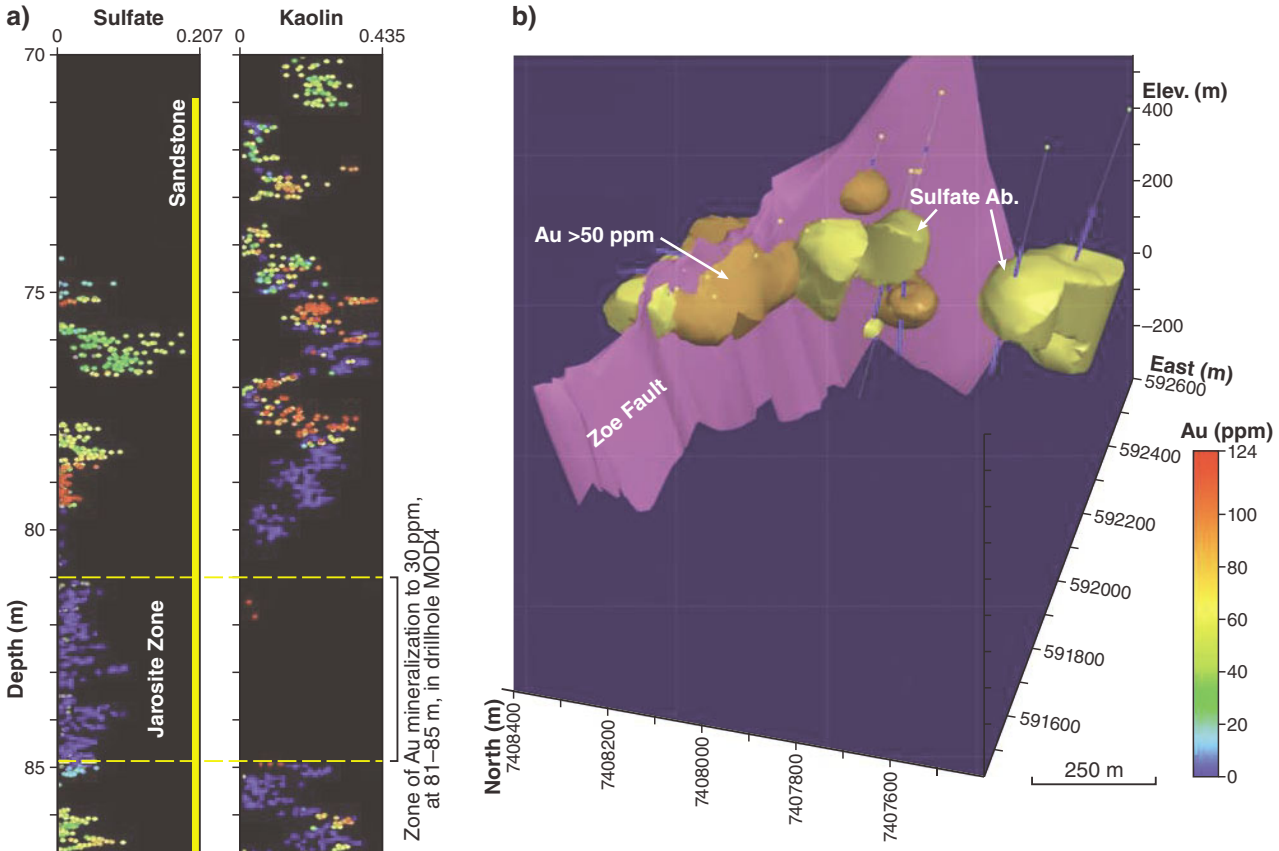

Figure 2. **a) Representative downhole plots of changes in the sulfate abundance (coloured by the sulfate mineral type) and kaolinite abundance (coloured by the Al-clay type) in relation to reported gold grades at Mt Olympus, using as an example, drill hole MOD4 over the interval 70–95 m depth; b) elevated perspective view (plunge +020°, azimuth 073°) of Mt Olympus looking due east. The steeply inclined, northwest-southeast striking Zoe Fault (lilac) is the most significant structural feature mapped in the area. Modelled isovolumes define the highest sulfate abundance (yellow) and gold zones (>0.5 ppm). Sandstone at 71–90 m, was the major lithology logged for the depth interval shown.**

Figure 3. **(opposite) Comparison of AEM and ASTER geoscience products, Mount Olympus area: a) bedrock geology (grey — Shingle Creek Group; pink — Wyloo Group), locations of HyLogging-3 data (e.g. NMD004). AEM lines FID59 and FID60 intersect major structural or lithological boundaries (NF-Nanjilgardy Fault; OF1-Fault at southern contact between Shingle Creek and Wyloo Groups, LCN-Fault at northern contact between the Shingle Creek and Wyloo Group; b) and c) ASTER 'MgOH Group Content' product (blue — low content, red — high content) over greyscale digital elevation model (DEM). The red box outline in b) shows the 'MgOH Group Content' mapped in c); d) conductivity-depth sections from a smooth model (30-layer), inversion of TEMPEST data along AEM line FID59. Solid, vertical black lines (without arrowheads) show locations of the NF and the contacts between lower and upper Wyloo Group (OF1, LCN) in the AEM and ASTER geoscience product map. Three additional sharp, conductivity highs are evident between OF1 and NF (pink arrows), which all can be extrapolated to the East and West using the 'MgOH Group Content' image.**

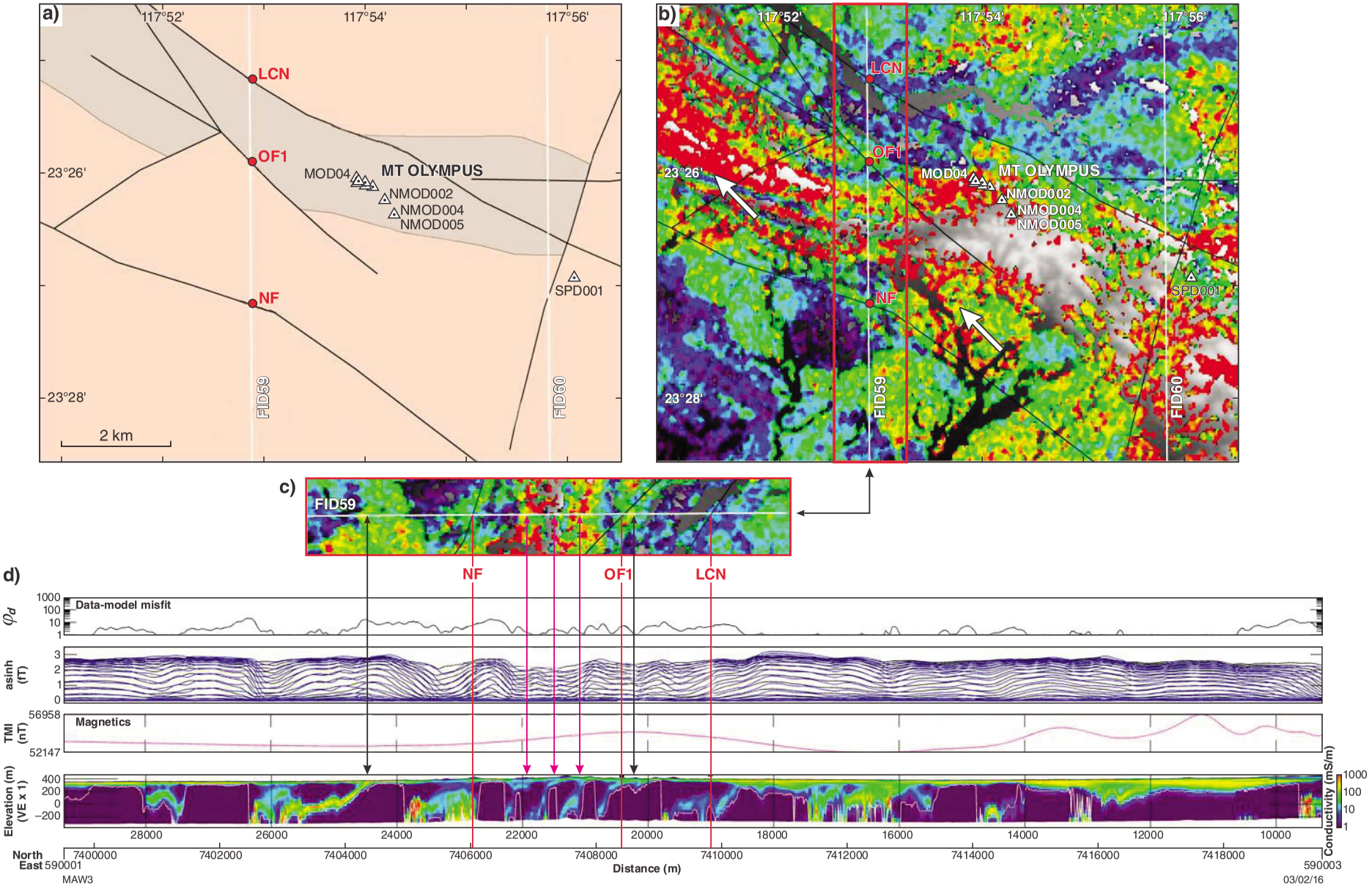
a)
117°52'
117°54'
117°56'
LCN
OF1
23°26'
MOD04
MT OLYMPUS
NMOD002
NMOD004
NMOD005
SPD001
NF
23°28'
FID59
FID60
2 km
b)
117°52'
117°54'
117°56'
LCN
OF1
23°26'
MOD04
MT OLYMPUS
NMOD002
NMOD004
NMOD005
SPD001
NF
23°28'
FID59
FID60
c)
FID59
NF
OF1
LCN
d)
Data-model misfit
asinh (fT)
Magnetics
TMI (nT)
56958
52147
Elevation (m) (VE x 1)
Conductivity (mS/m)
28000
26000
24000
22000
20000
18000
16000
14000
12000
10000
North
East
7400000
7402000
7404000
7406000
7408000
7410000
7412000
7414000
7416000
7418000
590001
590003
Distance (m)
MAW3
03/02/16

Such spatial changes in the white mica and chlorite composition may reflect hydrothermal overprinting of earlier metamorphic patterns within proximity to the Zoe Fault. In addition, the presence of other fault surfaces not mapped or recognized, may also play a role and lithological changes (e.g. siltstone, conglomerate, sandstone) can impact on the composition of the hydrothermal alteration mineral assemblages. In general, the extent of the hydrothermal mineral footprints is only on the metre to decametre scale.

Distal footprint alteration mineralogy

Comparison of HyLogger-3 data with ASTER surficial data, constrained by GSWA regolith geochemistry and inversion modelling of airborne electromagnetic (AEM) data along selected TEMPEST flight lines at Mt Olympus, was undertaken to evaluate the potential for gold-related alteration or structural indicators to be detected remotely. ASTER mineral products, such as the 'MgOH Group Content' (Cudahy et al., 2012) showed patterns that could be correlated with pervasive chlorite (±white-mica) assemblages or major structures, interpreted as distinct, conductive, subsurface geological domains in the AEM data (Fig. 3).

Several sharp, east-trending conductivity highs were modelled between larger structures, such as the NF and OF1 faults (Fig. 3), which coincided with increased ASTER 'MgOH Group Content' index values. These features may be smaller-scale structures not previously identified by geological mapping (e.g. faults, lithological contacts, bedding-parallel shear zones). Additionally, a well-defined conductivity contrast south of the NF, may indicate another significant structure not recognized by previous geological mapping, although there were no corresponding changes in the ASTER 'MgOH Group Content' index. Correlation between ASTER geoscience products and surface geochemical data was only evident using the relatively coarsely spaced, GSWA regional regolith sampling. For example, peaks in the ASTER 'Silica Index' broadly coincided with elevated wt% SiO_2 contents in the GSWA regolith geochemistry data, and were related to distinct lithologies.

Conclusion

Drillcore hyperspectral characterization of the alteration mineralogy associated with gold mineralization at Mt Olympus successfully identified four gold mineralization types and associated alteration footprints. Potential hydrothermal alteration phases were represented by (proximally) Na/K-alunite, well-ordered kaolinite, dickite and pyrophyllite (indicative of advanced argillic alteration); muscovite (indicative of phyllic alteration); Fe/Mg-chlorite and carbonate (distally), which were also mapped to varying extents at the surface using a field-portable VNIR-SWIR spectroradiometer. Whilst this apparent patchy Fe, K, Na, Al and S metasomatic alteration zonation showed some relationship to local structural features, and as was reflected at the deposit scale in ASTER mineral product mapping of the area around Mt Olympus, evidence for significant alteration zonation associated with the Nanjilgardy Fault could not be found in the multispectral remote sensing data. However, coarse-resolution, multispectral platforms, such as ASTER, may not have the required sensitivity either spectrally or spatially to detect alteration systems with a limited footprint. Future exploration programs may benefit from using commercially available airborne hyperspectral data or soon-to-be-launched hyperspectral satellites (e.g. EnMAP) for detecting potential, small-scale alteration associated with large-scale structures, such as the Nanjilgardy Fault.

References

Cudahy, T, Caccetta, M, Lau, I, Rodger, A, Laukamp, C, Ong, C, Chia, J, Collings, S, Rankine, T, Fraser, R, Woodcock, R, Vote, J, Warren, P, Thomas, M, Tyler, I, Mauger, A, Close, D, Jones, M, and Abrams, M 2012, Satellite ASTER geoscience map of Australia, Version 1: CSIRO Australia, Data Access Portal, <https://data.csiro.au/dap>, doi:10.4225/08/51400D6F7B335.

Hough, R 2015, Distal footprints of giant ore systems: Capricorn case study, *in* GSWA 2015 extended abstracts: promoting the prospectivity of Western Australia: Geological Survey of Western Australia, Record 2015/2, p. 9–12.

Johnson, SP, Thorne, AM, Tyler, IM, Korsch, RJ, Kennett, BLN, Cutten, HN, Goodwin, J, Blay, O, Blewett, RS, Joly, A, Dentith, MC, Aitken, ARA, Holzschuh, J, Salmon, M, Reading, A, Heinson, G, Boren, G, Ross, J, Costello, RD and Fomin, T 2013, Crustal architecture of the Capricorn Orogen, Western Australia and associated metallogeny: Australian Journal of Earth Sciences, v. 60, p. 681–705.

Morant, P and Doepel, MG 1997, The Mount Olympus gold deposit, *in* Combined mineral exploration report GSWA reference C451/1996, Ashburton project, Southeastern exploration area, Dublin Hill JV and related tenements, 1997 Annual report (part A), Perth, Western Australia, 10p.

Pirajno, F 2004, Metallogeny in the Capricorn Orogen, Western Australia, the result of multiple ore-forming processes: Precambrian Research, v. 128, p. 411–439.

Şener, AK, Young, C, Groves, DI, Krapež, B and Fletcher, IR 2005, Major orogenic gold episode associated with Cordilleran-style tectonics related to the assembly of Paleoproterozoic Australia: Geology, v. 33, no. 3, p. 225–228.

Tyler, IM and Thorne, AM 1990, The northern margin of the Capricorn Orogen, Western Australia — an example of an Early Proterozoic collision: Journal of Structural Geology, v. 12, no. 5/6, p. 685–701.

Tyler, IM, Johnson, SP, Thorne, AM and Cutten, HN 2011, Implications of the Capricorn deep seismic survey for mineral systems, *in* Capricorn Orogen seismic and magnetotelluric (MT) workshop 2011: extended abstracts *edited by* SP Johnson, AM Thorne and IM Tyler: Geological Survey of Western Australia, Record 2011/25, p. 115–120.